Renewable Energy 222 (2024) 119881

Contents lists available at ScienceDirect

Renewable Energy

journal homepage: www.elsevier.com/locate/renene

Effect of air equivalence ratio on the characteristics of biomass partial gasification for syngas and biochar co-production in the fluidized bed

Deao Zhu [a,b], Qinhui Wang [a,b,*], Guilin Xie [a,b], Zefu Ye [c], Zhujun Zhu [c], Chao Ye [d]

[a] State Key Laboratory of Clean Energy Utilization, Zhejiang University, Hangzhou, Zhejiang, 310027, China
[b] Key Laboratory of Clean Energy and Carbon Neutrality of Zhejiang Province, Zhejiang University, Hangzhou, Zhejiang, 310027, China
[c] Shanxi Gemeng US-China Clean Energy R&D Center Co. Ltd, Taiyuan, Shanxi, 030032, China
[d] Department of Energy and Environmental System Engineering, Zhejiang University of Science and Technology, Hangzhou, Zhejiang, 310023, China

ARTICLE INFO

Keywords:
Biomass
Partial gasification
Air equivalence ratio
Co-producting of syngas and biochar
Fluidized bed

ABSTRACT

In order to explore the characteristics and mechanism of biomass partial gasification for biochar and syngas co-production in the fluidized bed, a study on the influence of gasification performance and biochar characteristics after partial gasification with different air equivalence ratios was carried out in a self-built small atmospheric bubble fluidized bed. The results indicate that when the air equivalence ratio rises from 0.07 to 0.16, the lower calorific value of wet producer gas keeps decreasing, and the maximum value can reach 9.16 MJ/Nm^3. The biochar yield shows a declining trend, and the maximum value is 18.07 %. In addition, when the air-equivalence ratio is lower than 0.14, the rising of air equivalence ratio makes biochar more disordered due to the newly formed C–O structures, and the total Raman intensity will thereby continue to increase.

1. Introduction

In the context of carbon peak and carbon neutrality, the energy utilization of biomass with characteristics of natural carbon neutrality and zero carbon emission is receiving increasing attention. In China, the biomass resources have great potential for development [1–3], but there is still a problem of insufficient energy utilization rate [4,5]. the natural degradation after being discarded in large quantities and open burning cause serious environmental pollution, so there is an urgent need for energy utilization technologies that can handle a great deal of biomass.

Biomass gasification technology is a highly efficient energy utilization technology that is becoming mature and used extensively. From the concept, it is a thermochemical process that converts biomass into valuable producer gas, tar and biochar under high-temperature (>500 °C) and anoxic conditions. Traditional biomass gasification aims to convert low-quality biomass waste into valuable producer gas as much as possible in pursuit of high conversion rate and high efficiency, while paying little attention to the biochar, a byproduct in the gasification process [6].

In recent years, biochar has been widely applied in many areas [7–9], including as adsorbent [10,11], raw material for gasification [12] and catalyst [13,14] or using in electrochemistry [15,16] and soil improvement [17,18], and its value-added exploitation has been realized. At present, biochar is mainly produced by pyrolysis and gasification, but the use of gasification technology for biochar production is increasingly attached importance due to the long time and external heat source required for the production of biochar by pyrolysis [19] and the high economic feasibility of gasification, which helps to improve the physicochemical properties of biochar and allows continuous feedstock feeding [9]. In this case, Zhejiang University proposed relevant technologies based on biomass partial gasification for biochar and syngas co-production in the fluidized bed, whose technical routes are shown in Fig. 1. In this process, biomass particles are transported into a fluidized bed gasifier together with gasifying agent for partial gasification coproducing producer gas, tar and biochar, of which uncondensed and gaseous tar together with producer gas are sent to the boiler for combustion to achieve biomass partial gasification in fluidized bed coupled with coal-fired power generation or sent to the combustion chamber for combustion to recover waste heat producing steam to achieve biomass partial gasification for biochar and steam co-production in the fluidized bed. At present, the industrial plant for biochar co-production from agricultural and forestry waste-based partial gasification in fluidized bed coupled with coal-fired power generation is under construction, and the technology of biomass partial gasification for biochar and steam co-production in the fluidized bed has achieved industrial application for a wide range of feedstocks. So it is crucial to study the characteristics

* Corresponding author. State Key Laboratory of Clean Energy Utilization, Zhejiang University, Hangzhou, Zhejiang, 310027, China.
E-mail address: qhwang@zju.edu.cn (Q. Wang).

https://doi.org/10.1016/j.renene.2023.119881
Received 28 April 2023; Received in revised form 7 December 2023; Accepted 21 December 2023
Available online 22 December 2023

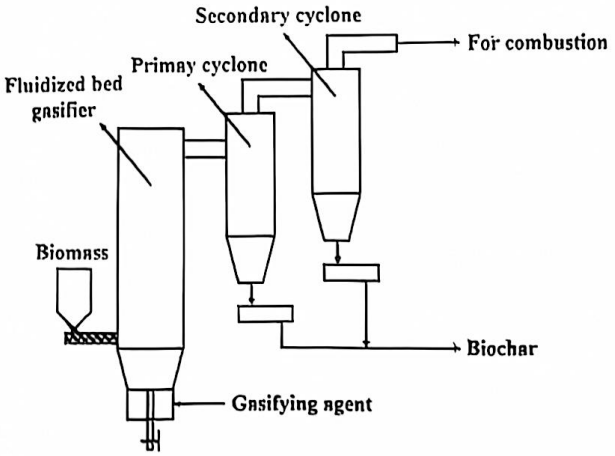

Fig. 1. Technical route schematic diagram of relevant technologies based on biomass partial gasification for biochar and syngas co-production in the fluidized bed.

and mechanisms of biomass partial gasification for biochar and syngas co-production to further reduce carbon emission and save energy to enhance the economics of related technology.

Xiao Feng [20] et al. proposed a biomass partial gasification model based on the principle of energy cascade utilization, and conducted thermodynamic and economic analysis of the model based on different key parameters. The results showed that when biomass gasification took syngas and biochar as output products, exergy efficiency could reach 67.97 %. The initial capital cost of biomass partial gasification process was 12.93 % less than complete biomass gasification process. This indicates that the technology of biomass partial gasification for biochar and syngas co-production has great application prospects. Yao [21] et al. developed a coupled RPM and fixed-bed gasification model in which the fixed-bed reactor was divided into three zones to simulate heat and mass transfer in order to predict the effect of different equivalence ratios on the syngas and biochar co-production characteristics of fixed-bed gasification, and the results indicated that the calorific value of syngas and biochar yield both had a decreasing trend with the increasing air equivalence ratios, and the largest calorific value of syngas could reach up to 6.15 MJ/Nm^3 and the maximum biochar yield was 22 %. AMJ Rivas [22] et al. studied the effect of different airflow rates on the generation of both syngas and biochar from rice hull and wood chip gasification in a top-lit updraft gasifier, and the results suggested that the calorific value of syngas generated from rice hull and wood chip had little difference with the increase of airflow rates, and the highest biochar yield from rice hull and wood chip were 39.3 % and 27.1 % respectively. Yimeng Zhang [23] et al. investigated the characteristics of downdraft fixed-bed gasification for biochar and syngas co-production in 3 MW project of apricot shell gasification power generation co-production of activated carbon, heat and fertilizer, and the results revealed that the highest calorific value of syngas and biochar yield were 4.9 MJ/Nm^3 and 25.9 % separately. However, the above studies mostly focus on partial gasification for biochar and syngas co-production in the fixed bed, and there is currently a lack of research content on biomass partial gasification for biochar and syngas co-production in the fluidized bed.

In addition, from the point of view of the reaction rate change law during the biomass gasification process in the existing literature analysis and the principle of energy cascade utilization, it is more advantageous to achieve biomass partial gasification for biochar and syngas co-production at low temperatures than at high temperatures. On the one hand, the temperature below 700 °C can minimize the loss of chemical energy [24,25], and on the other hand, it can avoid the problems of sintering, agglomeration and deposit corrosion that can occur at high temperatures [26].

Furthermore, since air is cheaper than other gasification agents [25] and the air equivalence ratio and gasification temperature in the operation of industrial biomass gasification plants are in one-to-one corresponding relations, the experiments on air gasification of biomass are conducted in a self-built small atmospheric bubble fluidized bed to investigate the characteristics and mechanism of biomass partial gasification for biochar and syngas co-production under different air equivalence ratios, so as to supply a data base to relevant technologies based on biomass partial gasification for biochar and syngas co-production in the fluidized bed.

2. Materials and methods

2.1. Materials

As one of the fastest growth rate tree species, poplar, is widely planted in most areas of China. Although it is not a common forestry biomass in gasification feedstock, it has excellent potential for energy production [27]. Therefore, the biomass used in this experiment is poplar sawdust, whose proximate and ultimate analysis and calorific value are shown in Table 1. In addition, the quartz sand is the bed material used in this experiment. Before the experiment, the poplar sawdust samples are screened to the particle size range from 0.45 mm to 0.9 mm, and the quartz sand bed materials are sieved to the particle size range from 0.2 mm to 0.45 mm. After screening, the poplar sawdust and quartz sand are dried at 105 °C for 12 h and sealed for use.

2.2. Experimental system

The partial gasification experiments of poplar sawdust are carried out in a self-built small atmospheric bubbling fluidized bed reactor. The experimental system is shown in Fig. 2. The system mainly includes fluidized bed reactor, biomass feeding system, air supply system, gas preheating device(5# and 6#), cyclone separation system, induced draft fan and distributed control system(DCS). The furnace body is made of ceramic, with an inner diameter of 120 mm and a height of 2600 mm. Four groups of resistance heating wires (1#, 2#, 3# and 4#) are wrapped around the furnace to preheat it to reduce local heat loss. Meantime, the aluminum silicate insulation cotton and high-temperature cement are wrapped around the furnace to improve the thermal insulation capacity of the furnace, and the outermost layer is steel shell. Poplar sawdust is supplied by screw feeder, and its frequency is controlled by DCS system. The air is input by a centrifugal fan, measured by a flowmeter, and heated by two preheaters before being fed into the furnace. The cyclone separation system consists of a two-stage cyclone separator to collect the biochar produced by partial gasification for further analysis.

2.3. Experimental methods

The partial gasification experiments of poplar sawdust in fluidized bed are carried out according to the following steps: (1) Start the electric heating device and gas preheating device for the furnace, and set their temperatures at 600 °C and 200 °C respectively. Meanwhile, open the low-temperature ethanol thermostat bath, and set its temperature at −40 °C. (2) When the temperature rises to the specified temperature, add 1800 mL (about 2.0 kg) quartz sand into the furnace, and open the centrifugal fan, introduce atmospheric air into the furnace to ensure that the bed material is fully fluidized. (3) When the temperature rises again, add poplar sawdust samples to the biomass spiral feeder, and open the spiral feeder to set a certain feeding frequency, so that feed poplar sawdust into the furnace. The gasification temperature required by the experimental condition is adjusted by the air-biomass ratio. Moreover, set the temperature of resistance heating wires to the average temperature of the furnace. (4) When the partial gasification is in a stable

Table 1
The proximate and ultimate analysis and lower calorific value of poplar sawdust.

Ultimate Analysis/(wt%)					Proximate Analysis/(wt%)				$Q_{net,ad}$
C_d	H_d	N_d	$S_{t,d}$	O^*_d	M_{ad}	A_{ad}	V_{ad}	FC_{ad}	MJ/kg
49.65	5.81	0.22	1.69	41.26	2.92	1.33	80.76	14.99	20.25

Note: ad: air dried basis. d: dry basis. *: by subtraction.

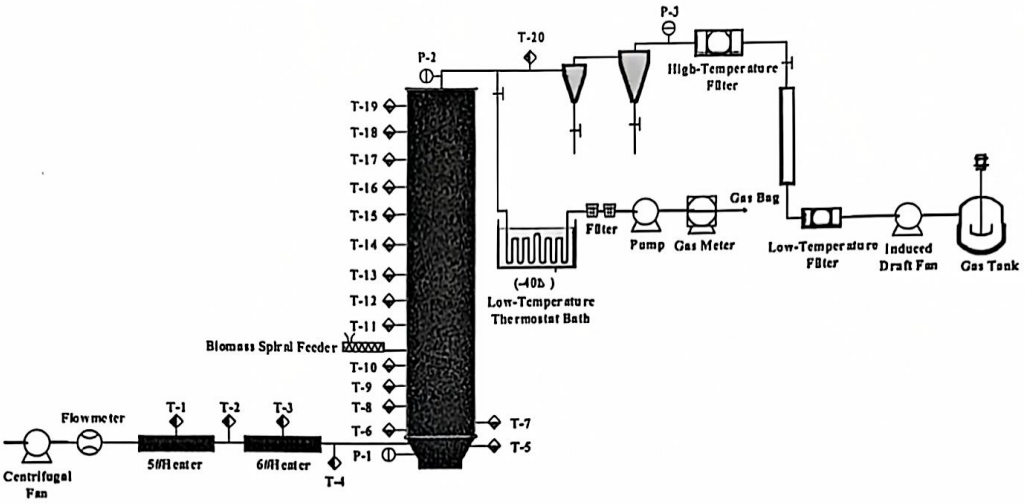

Fig. 2. Schematic diagram of the experimental system.

condition, start tar sampling, and the purified producer gas samples are collected at a 10-min interval, and the results of producer gas components are averaged. (5) After 30-min stabilized operation, shut down the spiral feeder, electric heating device and gas preheating device, and the air is still sent into furnace to cool it. When the furnace cools to below 150 °C, shut down the centrifugal fan and electric cabinet.

The partial gasification products studied in this experiment mainly include producer gas, biochar and tar. The producer gas dried samples are collected by gas sampling bag, and the main components in the producer gas are analyzed quantitatively by gas chromatography (GC, Agilent 7890BGC). The gas chromatography contains two thermal conductivity detectors (TCD) and a hydrogen flame ionization detector (FID). The thermal conductivity detector are used to detect CO, CO_2, CH_4, O_2, N_2 and H_2, and the hydrogen flame ionization detector is used to detect CH_4, C_2H_4, C_2H_6, C_3H_6 and C_3H_8. The temperature of these detectors are 200 °C, and the volume fraction of C_nH_m are the sum of C_2H_4, C_2H_6, C_3H_6 and C_3H_8. Biochar is mainly separated and released by a two-stage cyclone separator and collected by a N_2 cooled container to prevent further oxidation of high-temperature biochar when it encounters air. The physicochemical property analysis of biochar mainly includes the proximate and ultimate analysis, the lower calorific value analysis, pore characteristic, internal carbon morphology and O-containing chemical structure. The pore characteristics are analyzed by a specific surface area analyzer (Micromeritics APSP 2460) for nitrogen adsorption and desorption testing to identify the pore structure. The internal carbon morphology are determined by Raman spectrometer (Thermo Scientific DXR 3Xi) to analyze its carbon microstructure and crystal structure. The O-containing structure are determined by X-ray photoelectron spectroscopy (Thermo fisher Nexsa). Tar samples are collected by graham condenser, filter and silicone tube, etc., and the mass of sampling device before and after is recorded. The moisture contents of the producer gas are determined by Karl Fischer Moisture Titrator (ZDJ 2S), the weight of biochar collected by the tar sampling unit is determined by the quality difference of the filter paper before and after the filtering, and the tar content is obtained by the subtraction.

The specific experimental conditions are shown in Table 2, in which the biomass feeding frequency is fixed, and the change of air equivalence ratio is realized by changing the flow rate of air. The air equivalence ratio (ER) is between 0.07 and 0.16. The gasification temperature (T) is monitored and expressed by the thermocouple T-9 inserted into the dense phase zone of the furnace in Fig. 2.

Table 2
Experimental conditions.

Experimental condition	1	2	3	4	5
ER	0.07	0.09	0.12	0.14	0.16
T/°C	602	634	673	689	716

2.4. Related index calculation

After the experiment, relevant indexes are calculated according to the sampling analysis results of the products. The calculation method is as follows:

(1) The air equivalence ratio

The air equivalence ratio refers to the ratio between the actual supply of air during biomass partial gasification and the theoretical amount of air required for complete combustion of biomass. The calculation formula is as follows:

$$ER = \frac{V_{air}}{M_{Biomass} \times (Air/Biomass)_{stoic}} \quad (1)$$

Where, ER refers to the air equivalence ratio, V_{air} (Nm^3) refers to the total volume of air feeding into the furnace in the stabilized condition, $M_{Biomass}$ (kg) refers to the total mass of biomass feeding into the furnace in the stabilized condition, and $(Air/Biomass)_{stoic}$ (Nm^3/kg) refers to the theoretical air-to-fuel ratio required for the complete combustion of biomass per unit mass.

(2) gas yield

Gas yield refers to the volume of producer gas produced by gasification of biomass per unit mass under standard state. As N_2 generated from biomass partial gasification is negligible compared with N_2 injected by gasification agent, N_2 tracer method [28] can be used to calculate the gas yield. The calculation formula is as follows:

$$G_V = \frac{V_{air} \cdot X_{N_2air}}{M_{Biomass} \cdot X_{N_2gas}} = \frac{V_0}{M_{Biomass}} \quad (2)$$

Where, G_V (Nm^3/kg) is the gas yield, X_{N2air} (%) and X_{N2gas} (%) are the volume fraction of nitrogen in the air and in the wet producer gas respectively, V_0 (Nm^3) is the volume of wet producer gas.

(3) The lower calorific value of wet producer gas

The lower calorific value of wet producer gas refers to the chemical energy contained in the unit volume of producer gas, which can be calculated according to the lower calorific value of combustible components in wet producer gas. Since the moisture content of the feeding air is 0.03 %, which is negligible, the moisture content of producer gas detected by the above sampling is used as the wet basis for the gas composition. The formula for calculating the lower calorific value of wet producer gas is as follows:

$$Q_{rd} = \sum X_j \times q_j \quad (3)$$

Where, Q_{rd} (MJ/Nm^3) is the lower calorific value of wet producer gas, X_j is the volume fraction of combustible component j (H_2, CO, CH_4, C_2H_4, C_2H_6, C_3H_6, C_3H_8) in wet producer gas, and q_j (MJ/Nm^3) is the lower calorific value of component j.

(4) Carbon conversion ratio of the producer gas to biomass

Carbon conversion ratio of the producer gas to biomass refers to the ratio of carbon content in producer gas to carbon content in biomass. the calculation formula is as follows:

$$\varphi_{GC} = \frac{12 \times G_V \times \sum X_n}{22.4 \times C_{Biomass}} \times 100\% \quad (4)$$

Where, φ_{GC} (%) represents carbon conversion ratio of the producer gas to biomass, X_n represents the volume fraction of CO, CO_2, CH_4, 2 times C_2H_4, 2 times C_2H_6, 3 times C_3H_6 and 3 times C_3H_8 in wet producer gas, and $C_{Biomass}$ represents the carbon mass fraction in biomass.

(5) gasification efficiency

Gasification efficiency refers to the ratio of the chemical energy contained in the producer gas generated by the biomass gasification unit to the chemical energy contained in the biomass fuel added in the same time. The calculation formula is as follows:

$$\eta_q = \frac{Q_{rd} \times V_0}{Q_{Biomass} \times M_{Biomass}} \times 100\% \quad (5)$$

Where, η_q (%) is the gasification efficiency of biomass gasification unit, Q_{rd} (MJ/Nm^3) and $Q_{Biomass}$ (MJ/kg) are the lower calorific value of wet producer gas and biomass fuel respectively.

(6) biochar yield

Since all biochar samples cannot be collected during the experiment, ash balance method is adopted to calculate biochar yield to avoid errors. The calculation formula is as follows:

$$Y_{Biochar} = \frac{A_{Biomass}}{A_{Biochar}} \times 100 \quad (6)$$

Where, $Y_{Biochar}$ (%) is the yield of biochar, $A_{Biomass}$ (%) and $A_{Biochar}$ (%) are the ash content of biomass and biochar respectively. In order to avoid the oxidation of high-temperature biochar by air, the biochars used for ash content determination are collected from the tar sampling device.

(7) Carbon conversion ratio

The carbon conversion ratio of biomass partial gasification process is calculated by ash balance method. The calculation formula is as follows:

$$\eta_C = \left(1 - \frac{A_{Biomass} \times C_{Biochar}}{A_{Biochar} \times C_{Biomass}}\right) \times 100 \quad (7)$$

Where: η_C (%) is carbon conversion ratio, $C_{Biochar}$ (%) is carbon mass fraction of biochar, the biochars used for ash and carbon determination come from samples collected in tar sampling devices.

2.5. Gasification reaction

The chemical reactions involved in biomass partial gasification are very complex and mainly include two types, namely gas-solid non-homogeneous reactions and gas-phase reactions [29].

(1) gas-solid non-homogeneous reactions:

$2C + O_2 \rightarrow 2CO(\Delta H = -111\ kJ/mol)$ (R1)

$C + O_2 \rightarrow CO_2(\Delta H = -394\ kJ/mol)$ (R2)

$C + H_2O \rightarrow CO + H_2(\Delta H = +131\ kJ/mol)$ (R2)

$C + CO_2 \rightarrow 2CO(\Delta H = +172\ kJ/mol)$ (R4)

$C + H_2 \rightarrow CH_4(\Delta H = -75\ kJ/mol)$ (R5)

(2) gas-phase reactions:

$2H_2 + O_2 \rightarrow 2H_2O(\Delta H = -242\ kJ/mol)$ (R6)

$2CO + O_2 \rightarrow 2CO_2(\Delta H = -283\ kJ/mol)$ (R7)

$CO + H_2O \rightarrow CO_2 + H_2(\Delta H = -41\ kJ/mol)$ (R8)

$CH_4 + 2O_2 \rightarrow CO_2 + 2H_2O(\Delta H = -803\ kJ/mol)$ (R9)

$CH_4 + H_2O \rightarrow CO + 3H_2(\Delta H = +206\ kJ/mol)$ (R10)

$2C_nH_m + (2n + m/2)O_2 \rightarrow 2nCO_2 + mH_2O(exothermic)$ (R11)

$C_nH_m + nH_2O \rightarrow nCO + (m/2 + n)H_2(endothermic)$ (R12)

3. Results and discussion

3.1. Energy balance and carbon balance calculation

Because the heat loss of small experimental device is difficult to ignore, this experiment adopts the form of electric heating to make up part of the heat loss. In order to determine the compensatory effect of the experiment and industrial adaptability, the energy balance of the experimental results is calculated. The idea of energy balance calculation is to compare the input energy (excluding electric heating) and output energy (excluding heat dissipation) of the experimental system. The calculation is as follows:

$$Q_1 + Q_2 = Q_3 + Q_4 + Q_5 \quad (8)$$

Where, Q_1 (kJ) is the chemical energy of biomass in the feeding process, Q_2 (kJ) is the sensible heat of biomass in the feeding process and the sensible heat of air, Q_3 (kJ) is the chemical energy of dry producer gas and the sensible heat of dry producer gas and water vapor, Q_4 (kJ) is the chemical energy of tar and its sensible heat, Q_5 (kJ) is the chemical energy of biochar and the sensible heat of biochar and bed material.

The energy input items of the experimental system are calculated as follows:

$$Q_1 = M_{Biomass} \times Q_{Biomass} \times 1000 \quad (9)$$

$$Q_2 = M_{Biomass} \times C_{Biomass} \times T_{Biomass} + V_{air} \times C_{air} \times T_{air} \quad (10)$$

Where, $C_{Biomass}$ ($kJ \cdot kg^{-1} \cdot °C^{-1}$) and C_{air} ($kJ \cdot Nm^{3-1} \cdot °C^{-1}$) are the specific heat of biomass and air respectively, $T_{Biomass}$ (°C) and T_{air} (°C) are the temperature of biomass and air respectively.

The energy output items of the experimental system are calculated as follows:

$$Q_3 = Q_{gd} \times V_{gd} + V_{gd} \times \sum X_i C_i \times T_{producer\ gas} + V_{steam} \times C_{steam} \times T_{producer\ gas} \quad (11)$$

$$Q_4 = Q_{Tar} \times M_{Tar} + M_{Tar} \times C_{Tar} \times T_{producer\ gas} \quad (12)$$

$$Q_5 = M_{Biochar} \times Q_{Biochar} + M_{Biochar} \times C_{Biochar} \times T_{producer\ gas} + M_{bed} \times C_{bed} \times T \quad (13)$$

Where, Q_{gd} (kJ/Nm^3), Q_{Tar} (kJ/kg) and $Q_{Biochar}$ (kJ/kg) are the lower calorific value of dry producer gas, tar and biochar respectively, V_{gd} (Nm^3) and V_{steam} (Nm^3) are the volume of dry producer gas and water vapor respectively, X_i represents the volume fraction of dry producer gas component i(H_2, CO, CO_2, N_2, CH_4, C_2H_4, C_2H_6, C_3H_6 and C_3H_8), C_i ($kJ \cdot Nm^{3-1} \cdot °C^{-1}$), C_{steam} ($kJ \cdot Nm^{3-1} \cdot °C^{-1}$), C_{Tar} ($kJ \cdot kg^{-1} \cdot °C^{-1}$), $C_{Biochar}$ ($kJ \cdot kg^{-1} \cdot °C^{-1}$) and C_{bed} ($kJ \cdot kg^{-1} \cdot °C^{-1}$) is the specific heat of dry producer gas component i, water vapor, tar, biochar, and bed material separately, $T_{producer\ gas}$ (°C) and T (°C) are the temperature of producer gas and gasification temperature separately, M_{Tar} (kg), $M_{Biochar}$ (kg), M_{bed} (kg) are the mass of tar, biochar and bed material.

Experimental results of working condition 1 (corresponding to actual gasification temperature of 602 °C) and working condition 5 (corresponding to actual gasification temperature of 716 °C) are selected for energy balance calculation, as shown in Table 3. In the process of biomass partial gasification under low temperature, the ratio of system output energy to system input energy in working condition 1 and working condition 5 are 97.29 % and 94.73 %, respectively. As the error is basically less than 5 %, it indicates that the experiment has a good compensatory effect, and the experiment has a certain rationality and industrial feasibility. Due to the fact that all products generated by biomass partial gasification cannot be collected during the experiment, the specific heat of poplar sawdust in the energy balance is calculated according to the specific heat of poplar [30], the specific heat of tar is calculated according to the specific heat of benzene, the specific heat of dry producer gas and water vapor are calculated according to the specific heat capacity at constant pressure of component (H_2, CO, CO_2, N_2, CH_4, C_2H_4, C_2H_6, C_3H_6 and C_3H_8 and H_2O) in producer gas at gas temperature, and the specific heat of biochar and the calorific value of tar are calculated according to the empirical values given in literature [31, 32]. Therefore, the energy balance calculation can only estimate the energy input and output of the experimental system and verify that the electric heating makes up part of the heat loss.

Table 3
Energy balance calculation.

Items		602 °C	716 °C
Energy input	Q_1(kJ)	47592.20	47592.20
	Q_2(kJ)	226.75	480.13
Energy output	Q_3(kJ)	15283.77	22672.21
	Q_4(kJ)	17194.58	16885.26
	Q_5(kJ)	14042.90	5979.86
Energy output/Energy input*100(%)		97.29	94.73

In addition, in order to verify the accuracy of the experiment, the carbon balance is calculated for the experimental results. The idea of carbon balance calculation is to compare the sum of mass of carbon in producer gas, biochar and tar with the mass of carbon in biomass during the feeding process. The calculation is as follows:

$$MC_{Biomass} = MC_{Producer\ gas} + MC_{Biochar} + MC_{Tar} \quad (14)$$

Where, $MC_{Biomass}$ (kg), $MC_{Producer\ gas}$ (kg), $MC_{Biochar}$ (kg) and MC_{Tar} (kg) refers to the mass of carbon of biomass in feeding process, producer gas produced by biomass partial gasification, biochar and tar respectively.

The mass of carbon of the producer gas generated by biomass partial gasification is the sum of the carbon content of various carbon-containing producer gas components, which can be calculated as follows:

$$MC_{Producer\ gas} = \sum X_n \times V_0 \times 12/22.4 \quad (15)$$

The mass of carbon in biochar and tar are calculated according to the elemental analysis of biochar and tar as follows:

$$MC_{Biochar} = M_{Biochar} \times CMF_{Biochar} \quad (16)$$

$$MC_{Tar} = M_{Tar} \times CMF_{Tar} \quad (17)$$

Where, $M_{Biochar}$ (kg) and M_{Tar} (kg) are the mass of biochar and tar respectively, $CMF_{Biochar}$, CMF_{Tar} are the carbon mass fraction in biochar and tar respectively.

The experimental results of working condition 1 (corresponding to the actual gasification temperature of 602 °C) and working condition 5 (corresponding to the actual gasification temperature of 716 °C) are selected for carbon balance calculation, as shown in Table 4. In the process of biomass partial gasification under low temperature, the ratio of total carbon mass in producer gas, biochar and tar to input carbon mass of biomass in working conditions 1 and 5 are 99.20 % and 100.26 % respectively, indicating that the sample collection is complete and the experimental results are credible.

Although the feeding frequency of biomass feeder is the same under different working conditions, the actual mass of biomass fed into the furnace is affected by the pressure in the furnace, and there is a certain range of fluctuations. Furthermore, all the biomass partial gasification products cannot be collected during the experiment. Therefore, the mass of carbon of all products generated by the biomass partial gasification are not completely equal to the mass of carbon entering the gasifier.

3.2. Effect of air equivalence ratio on gasification performance

3.2.1. Effect of air equivalence ratio on gas components and component yield

Fig. 3 shows the variation law of wet producer gas components and component yield of poplar sawdust partial gasification under different

Table 4
Carbon balance calculation.

Items		601 °C	716 °C
Carbon input	$M_{Biomass}$(kg)	2.350	2.350
	MCBiomass (kg)	1.133	1.133
Carbon output	V0 (Nm^3)	1.503	2.675
	MBiochar (kg)	0.425	0.171
	MTar (kg)	0.469	0.455
	CMFBiochar	0.7884	0.5891
	CMFTar	0.7037	0.7388
	MCProducer gas (kg)	0.459	0.699
	MCBiochar (kg)	0.335	0.101
	MCTar (kg)	0.330	0.336
Carbon output/Carbon input*100 (%)		99.20	100.26

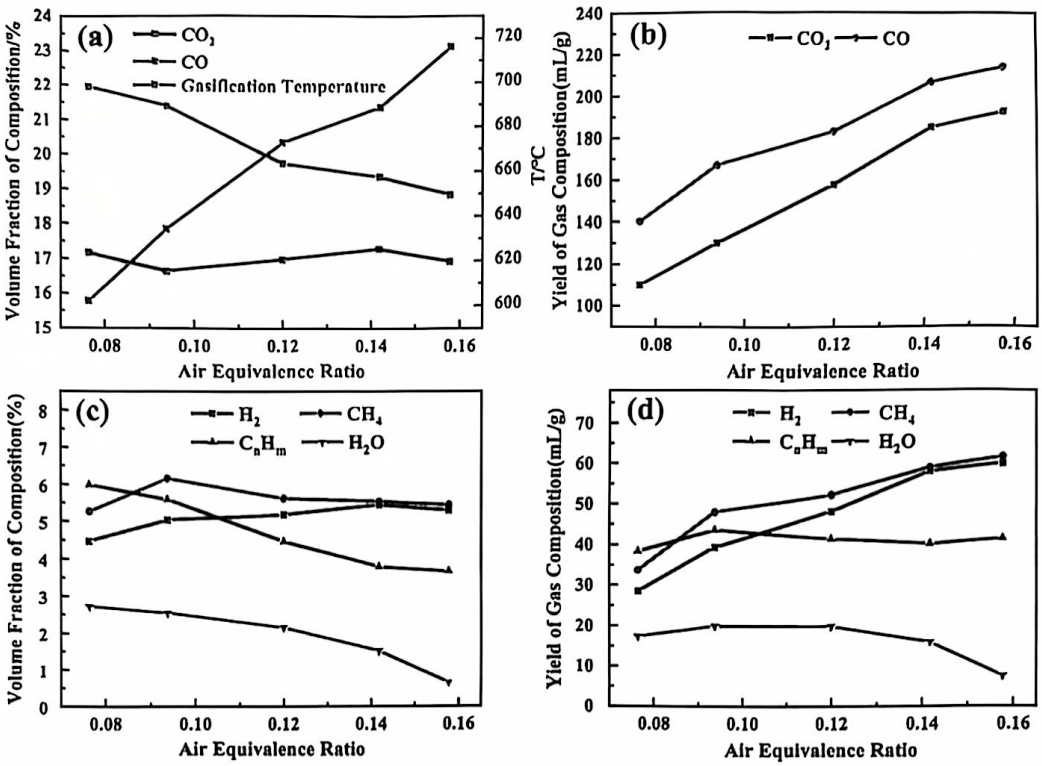

Fig. 3. Influence of equivalence ratio on components and yield of producer gas: (a) Volume fraction of CO and CO_2, Gasification Temperature, (b) Yield of CO and CO_2, (c) Volume fraction of H_2, CH_4, C_nH_m and H_2O, (d) Yield of H_2, CH_4, C_nH_m and H_2O.

equivalence ratios. The results show that the total content of combustible gas components including H_2, CH_4, CO and C_nH_m in the producer gas is between 33% and 39 %. At the same time, with the increase of equivalence ratio, the proportion of biomass reacting with oxygen gradually increases, and the released energy makes the gasification temperature rise continuously. As can be seen from the change of producer gas components in Fig. 3 (a), the volume content of CO decreases with the increase of equivalence ratio. The volume content of CO_2 shows a trend of first decreasing, then rising and then decreasing, but the range of change is not obvious. The CO mainly comes from exothermic reaction R1. The rise of temperature makes the reaction balance shift to the left, and the generation of CO is blocked. At the same time, with the rise of equivalence ratio, the reaction rate of reduction reaction R4 increases, which makes the growth rate of the late yield increase. However, as a whole, the slope of the change curve of CO yield in Fig. 3 (b) decreases continuously. Therefore, when the equivalence ratio rises from 0.07 to 0.16, the volume content of CO decreases continuously. For the CO_2, the decline in volume content in the early stage is mainly due to the dominance of pyrolysis at this stage. The yield of CH_4 rose sharply, and the yield of C_nH_m rose to the maximum. Therefore, the macro volume content of CO_2 decreases. The reason why the intermediate volume content increase with the equivalence ratio is that the reaction rate of combustion reactions R2, R9 and R11 increase with the rise of temperature. However, when the temperature continues to rise, the reduction reaction rate of R4 also continue to levate, resulting in a continuous reduction of CO_2, which could be verified by the slowing down of the growth rate of CO_2 yield in Fig. 3 (b).

The yield of hydrocarbon C_nH_m shows a trend of first increasing, then decreasing and then rising with the increase of equivalence ratio. On the one hand, hydrocarbon C_nH_m mainly comes from the pyrolysis of biomass materials. When the temperature increases, the yield increases to a certain extent, but when the temperature continues to rise, the reaction rate of the secondary decomposition reaction increases. In the reduction stage, the reaction rate of the combustion reaction R11 and the steam reforming reaction R12 also increase, so the subsequent yield decreases in Fig. 3 (d). On the other hand, when the temperature continues to rise, tar and linear hydrocarbons generated by gasification will undergo secondary cracking to generate C_nH_m. Meanwhile, literature [33] pointed out that the aromatic hydrocarbon and the adipose side chain of aliphatic hydrocarbon will decompose into C_2 around 700 °C, resulting in the recovery of C_nH_m yield in the later stage of the reaction. Owing to the volume proportion of C_nH_m is relatively small and the yield varies little, the volume fraction of C_nH_m decreases with the increase of equivalence ratio.

As can be seen from Fig. 3 (c), the volume content of CH_4 has an increasing-decreasing trend with the increasing equivalence ratio. On the one hand, the pyrolysis of biomass materials and the decomposition of hydrocarbons produce methane. When the equivalence ratio is 0.09, the pyrolysis dominates, so the yield increases sharply and the volume content increases. On the other hand, the reaction rate of R10 increases with the rise of temperature and the reaction equilibrium moves to the right, so the growth rate of its yield slows down. Therefore, under the counteraction of the two effects, the volume content of CH_4 shows a trend of increasing-decreasing with the increase of equivalence ratio.

The volume content of H_2 also has an increasing-decreasing trend with the increase of equivalence ratio. On the one hand, due to the constant rise of equivalence ratio and temperature, the reaction rate of R12 keeps increasing, thus promoting the increase of H_2 yield and volume content. On the other hand, with the further increase of equivalence ratio, H_2 will be consumed, which is consistent with the slower growth rate of the yield in the later period, thus reducing the volume content of H_2 in the later period.

It can be seen from Fig. 3 (c) and (d) that the increase of air equivalence ratio leads to the constant decline of volume content of H_2O, and the yield increases first and then decreases. On the one hand, the pyrolysis in the earlier stage is dominant, so the yield reaches the maximum when the equivalence ratio is 0.09. On the other hand, the increase of air equivalence ratio elevates the temperature and the

reaction rate of steam reforming reaction R10 and R12 and gives rise to the decrease of H_2O yield, which can be proved by the accelerated decline of the yield in the later stage. However, the increase of the yield in the earlier stage is not large, which leads to the reducing volume content.

3.2.2. Effect of air equivalence ratio on T, G_v and Q_{rd}

Fig. 4 shows the variation law of gasification temperature, gas yield and lower calorific value of wet producer gas under different equivalence ratios. The results indicate that the gasification temperature and gas yield are highly sensitive to the air equivalence ratio. As the air equivalence ratio continues to rise, the gasification temperature also continues to rise, mainly because the oxidation share of biomass gradually increases, more and more heat is released, and thus the temperature of the gasification system continues to rise. Meanwhile, the gas yield keeps rising with the increase of the air equivalence ratio, mainly due to the gas component yield except C_nH_m and H_2O keeps rising, which can be seen from the yield changes of each producer gas component in Fig. 3 (b) and (d), and the continuous air intake drives the gas yield to keep rising.

Since air is used as the gasification agent for partial gasification experiment, nitrogen is also introduced into the gasification system. As can be seen from Fig. 4, the increase of air equivalence ratio results in the decreasing of the lower calorific value of wet producer gas, but the change of the lower calorific value of wet producer gas in the early stage is not obvious. On the one hand, the increase of N_2 intake weakens the volume content of other combustible gases. On the other hand, the pyrolysis is dominant at this time, and more CH_4 and C_nH_m are produced, so the lower calorific value of wet producer gas has little change under the two effects. Compared with the biomass partial gasification at high temperature, the air equivalence ratio set in this experiment is lower, and the biomass pyrolysis share is larger. Therefore, the experimental lower calorific value of wet producer gas is higher. When the equivalence ratio is 0.07, the lower calorific value of wet producer gas is the highest, reaching 9.16 MJ/Nm^3.

3.2.3. Effect of air equivalence ratio on η_q and φ_{GC}

Fig. 5 shows the change rule of partial gasification efficiency and carbon conversion ratio of the producer gas to biomass under different equivalence ratios. The results demonstrate that with the continuous increase of air equivalence ratio, the gasification efficiency and carbon conversion ratio of the producer gas to biomass both show an upward trend, and the growth rate in the range of 0.07–0.09 is larger than that in the range of 0.09–0.16. The main cause is that the continuous increase of the air equivalence ratio promotes the rise of temperature and partial combustion of fixed carbon, thus motivating the conversion of more carbon in biomass into gas phase. As for the difference in growth rate, the main reason is that when the air equivalence ratio is below 0.09, air intake has a greater impact on the biomass partial gasification, while when the air equivalence ratio is above 0.09, the sensitivity of air to the biomass partial gasification is reduced, this also explains the feasibility of biomass partial gasification from another angle.

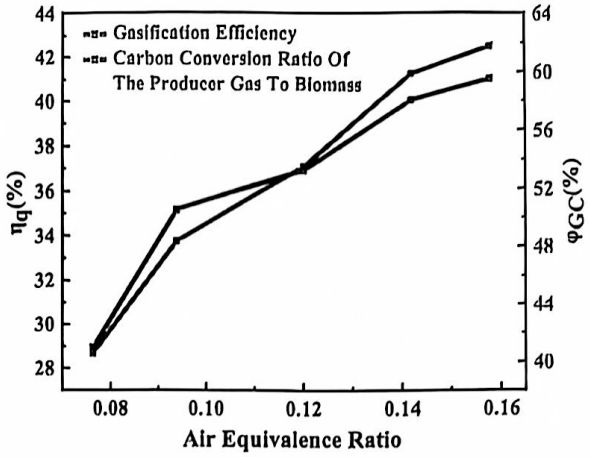

Fig. 5. Influence of equivalence ratio on gasification efficiency and carbon conversion ratio of the producer gas to biomass.

3.2.4. Effect of air equivalence ratio on characteristics of tar

Fig. 6 shows the variation of tar yield and carbon mass fraction of tar under different equivalence ratios. The results reveal that when the air equivalence ratio increases from 0.07 to 0.09, the tar yield increases from 19.94 % to 21.34 %, indicating that pyrolysis is dominant and the reaction rate of biomass pyrolysis to organic matter is the highest. When the air equivalence ratio further increases, the tar yield decreases from 21.34 % to 19.37 %, suggesting that the further increase of air supply promotes the secondary cracking and oxidation reaction of tar, resulting in the decrease of tar yield. In addition, the carbon mass fraction of tar reaches the maximum of 76.84 % when the air equivalence ratio is 0.14, and then decreases, which indirectly proves that the decomposition of light components in tar leads to an increase of the C_nH_m yield in the later producer gas.

3.3. Effect of air equivalence ratio on characteristics of biochar

Fig. 7 shows the change law of biochar yield, carbon mass fraction of biochar and carbon conversion ratio of partial gasification under

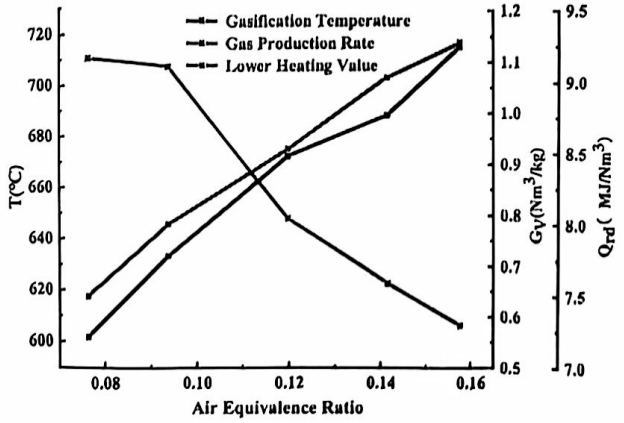

Fig. 4. Influence of equivalence ratio on gasification temperature, gas yield and lower calorific value of wet producer gas.

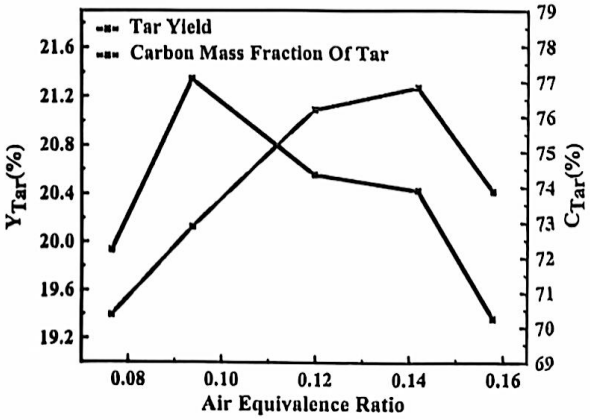

Fig. 6. Influence of equivalence ratio on tar yield and carbon mass fraction of tar.

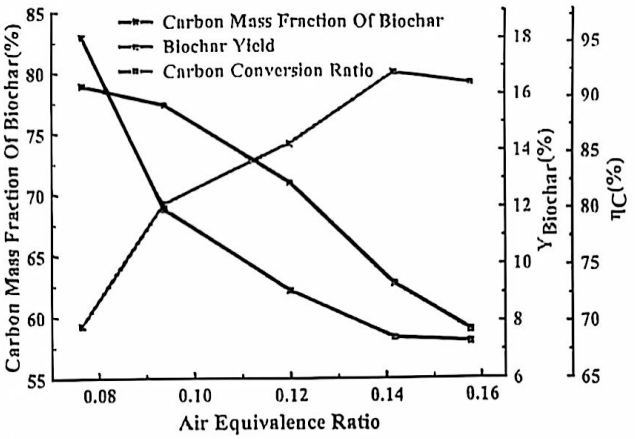

Fig. 7. Effect of equivalence ratio on biochar yield, carbon mass fraction of biochar and carbon conversion ratio.

different equivalence ratios. The results show that with the increase of air equivalence ratio, biochar yield decreases from 18.07 % to 7.28 %, carbon mass fraction of biochar drops from 78.84 % to 58.91 %. The increase of the air equivalence ratio promotes the reaction of more combustible components including carbon with oxygen to release more heat, the rapid precipitation of volatiles in biomass, partial combustion of fixed carbon and the conversion of more carbon in biomass into producer gas and tar, resulting in the continuous decline of biochar yield and carbon mass fraction of biochar. The carbon conversion ratio shows a trend of increasing-decreasing with the increase of air equivalence ratio. The main reason is that the increase in air supply contributes to the rise of temperature and partial combustion of fixed carbon, thus promoting the conversion of more carbon in biomass into producer gas and tar. However, with the further increase of air supply, the flue gas velocity in the inner section of the furnace increases, reducing the residence time of biochar particles produced by biomass partial gasification, and the biochar particles are blown out without sufficient reaction.

The variation patterns of proximate and ultimate analysis results of biochars from partial gasification of poplar sawdust at different air equivalence ratios are given in Table 5. The results show that when the air equivalence ratio increases from 0.07 to 0.14, the biomass particles react with more oxygen to release heat, the residual volatile fraction in the biochar gradually decrease from 16.82 % to 11.60 % and the fixed carbon content drop from 64.54 % to 52.36 %. The main reason is that the increase of air equivalence ratio leads to the increase of gasification temperature, which promotes the acceleration of volatiles precipitation and boosts the partial combustion share of fixed carbon. When the air equivalence ratio continues to rise, the residual volatile fraction in the biochar elevate, which also confirms the decrease of carbon conversion ratio in the later stage. In addition, the hydrogen content and H/C molar ratio in the biochar gradually descend with the rising of air equivalence ratio, mainly due to the consumption of lots of hydrogen atoms during the cracking and precipitation of macromolecular carbon chains in biomass.

Raman spectroscopy, as one of the most extensive and powerful analytical methods to characterize the evolution of carbon structure, can be used to analyze the internal carbon morphology of carbon-containing materials, especially biochar [34,35]. The internal carbon morphology of biochar is generally characterized by disordered structure (D peak) and graphitized structure (G peak). The original Raman spectra of biochar after partial gasification of poplar sawdust under different equivalence ratios are shown in Fig. 8. Biochar samples are labeled as biochar-1, Biochar-2, biochar-3, biochar-4, and biochar-5 in the following parts according to the equivalence ratio from low to high (gasification temperature from low to high). In general, peaks D and G overlap and some feature peaks are hidden. Therefore, in order to obtain more detailed information about internal carbon morphology, the five-peak fitting method (D1-D4, G) is generally adopted to carry out peak-differentiating and imitating for original Raman spectra, wherein Lorentz function is used to fit D1, D2, D4 and G peaks, and Gaussian function is used to fit D3 peak. The carbon morphology information represented by the five sub-peaks is shown in literature [36]. After peak fitting, the intensity of peaks in the Raman spectrum is represented by the integrated area of corresponding peaks, and the total peak intensity can be used to represent the degree of disordering of carbon-containing materials and to predict the existence of oxygen-containing functional groups. Fig. 9 (a) shows the change law of total peak intensity in the Raman spectrum of biochar generated by partial gasification under different equivalence ratios. The results demonstrate that with the increase of air equivalence ratio and gasification temperature, The total peak intensity of biochar have an increasing-decreasing trend, and reach the maximum value when the air equivalence ratio is 0.14 and the gasification temperature is 689 °C, indicating that when the air equivalence ratio is in the range of 0.07–0.14, increasing the air equivalence ratio improves the degree of biochar disorder. When the air equivalence ratio exceeds 0.14 and the gasification temperature reaches a certain degree, biochar becomes more orderly, which is consistent with the experimental results of Wang Shuai [37] et al. The main reason is that when the air equivalence ratio is in the range of 0.07–0.14, increasing

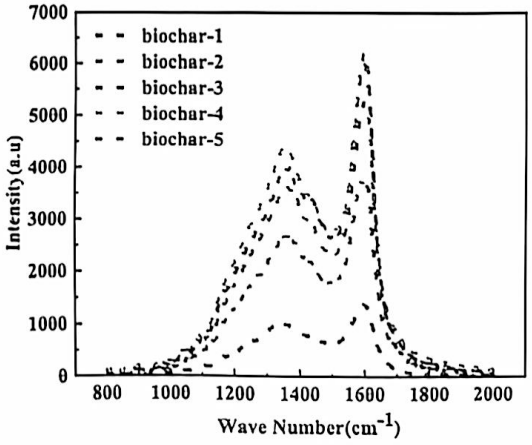

Fig. 8. Original Raman spectra of biochar at different equivalence ratios.

Table 5
The proximate and ultimate analysis of biochar under different ER.

Item	Ultimate Analysis/(wt%)					Proximate Analysis/(wt%)				H/C$_{mole}$
	C_d	H_d	N_d	$S_{t,d}$	O^*_d	M_{ad}	A_{ad}	V_{ad}	FC_{ad}	
1	73.45	2.25	0.49	0.18	6.62	1.97	16.67	16.82	64.54	0.37
2	66.87	1.95	0.44	0.18	5.70	2.54	24.22	15.02	58.22	0.35
3	59.10	1.67	0.32	0.39	5.49	1.25	32.61	13.14	53.59	0.34
4	58.98	1.52	0.35	0.40	3.98	1.94	34.10	11.60	52.36	0.31
5	53.41	1.38	0.12	0.31	7.41	1.29	36.89	14.34	50.37	0.31

Note: ad: air dried basis. d: dry basis. *: by subtraction.

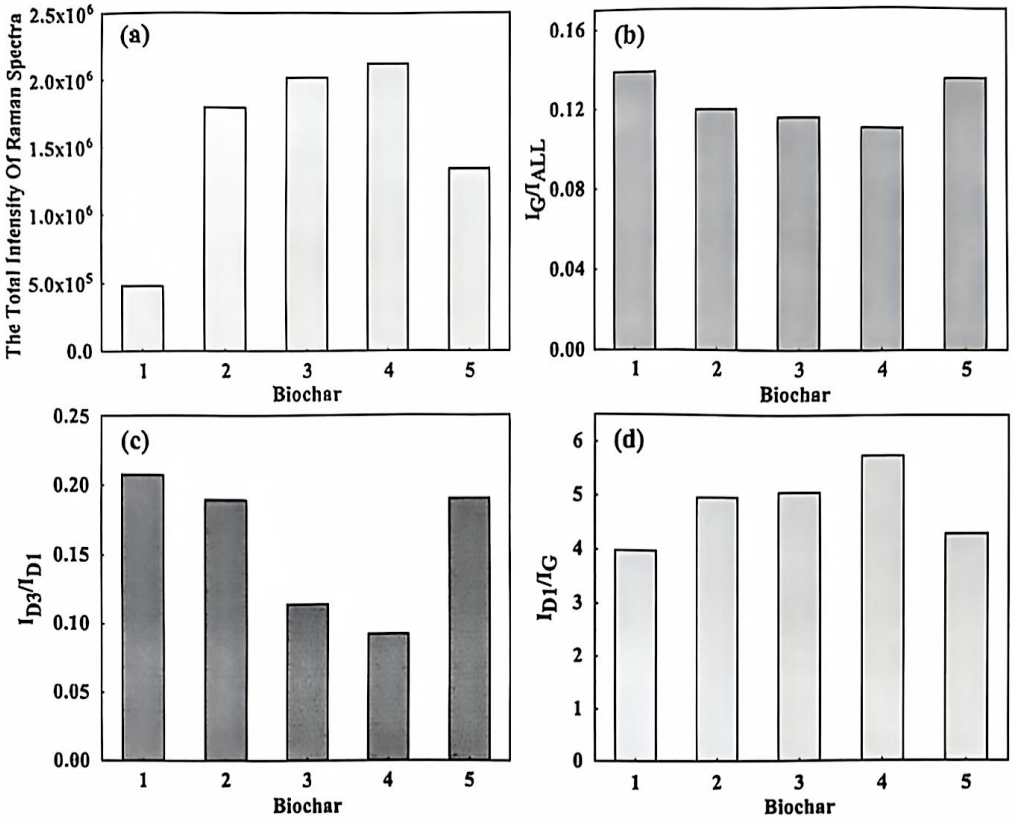

Fig. 9. Total peak intensity and sub-peak intensity ratios of biochar under different equivalence ratios: (a) Total peak intensity, (b) I_G/I_{ALL}, (c) I_{D3}/I_{D1}, (d) I_{D1}/I_G.

the air equivalence ratio makes biochar form additional oxygen-containing functional groups or aromatic compounds.

The peak intensity ratio of Raman spectra can also reveal the carbon structure of biochar. I_G/I_{ALL} can reveal the order degree of biochar, I_{D1}/I_G can reveal the disorder degree of biochar, and I_{D3}/I_{D1} represents the ratio of small aromatic compounds to large aromatic compounds. Fig. 9 (b) shows the variation law of I_G/I_{ALL} of biochar produced by partial gasification under different equivalence ratios. The results show that the ordered structure of biochar decreases first and then increases with the increase of air equivalence ratio, and a turning point occurs at the air equivalence ratio of 0.14, which also verifies the formation of additional oxygen-containing functional groups or aromatic compounds from another perspective. Fig. 9 (c) shows the variation law of I_{D3}/I_{D1} of biochar produced by partial gasification under different equivalence ratios. The results indicate that with the increasing of air equivalence ratio, I_{D3}/I_{D1} shows an decreasing-increasing trend. However, when the air equivalence ratio exceeds 0.14 and the gasification temperature reaches a certain degree, the large aromatic compounds are transformed into small aromatic compounds, and the I_{D3}/I_{D1} ratio rises again. Fig. 9 (d) shows the variation law of I_{D1}/I_G of biochar produced by partial gasification under different equivalence ratios. The results demonstrate that I_{D1}/I_G shows an increasing-decreasing trend with the increasing of air equivalence ratio, which is consistent with the carbon structure information revealed by I_G/I_{ALL}.

X-ray photoelectron spectroscopy (XPS), as one of the powerful analytical methods to characterize the elementary composition and chemical properties on the surface of biochar, can be used to analyze the concentration of carbon and oxygen species [38] and the chemical structure of oxygen-containing functional groups in the whole biochar during gasification [39]. In order to better study the mechanism of

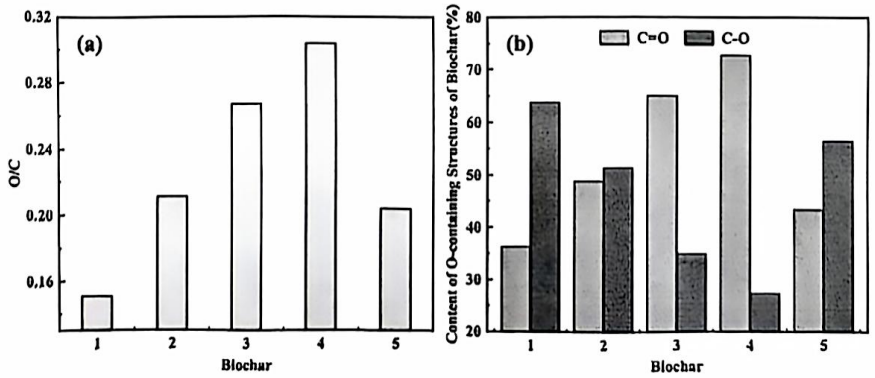

Fig. 10. Distribution of O/C ratio and relative oxygen-containing structure content of biochar under different equivalence ratios: (a) O/C, (b) relative oxygen-containing structure content.

partial gasification of poplar sawdust in air atmosphere at low temperature, XPS is used to characterize biochar under different air equivalence ratios. Fig. 10 (a) shows the change rule of O/C ratio of biochar generated by poplar sawdust partial gasification under different equivalence ratios. The results show that the O/C ratio of biochar first increases and then decreases with the increase of air equivalence ratio, which also indicates that additional oxygen-containing structures are formed during the process of low-temperature partial gasification based on air from another perspective. In order to further determine the detailed quantitative information of oxygen-containing structures in biochar and the additional oxygen-containing structures formed, the high-resolution O1s spectrum of biochars are deconvolution processed by Avantage software into two peaks, respectively representing C]O structure and C–O structure. The results of high-resolution O1s spectral processing by biochar-2 are shown in Fig. 11 below. Fig. 10 (b) shows the detailed changes of the relative oxygen structure content of biochar produced by partial gasification under different equivalence ratios. The results show that with the increasing of the air equivalence ratio, the C]O structure firstly increases and then decreases, while the C–O structure firstly decreases and then increases, which is consistent with the relevant experimental results of Wang Shuai [38] et al. Based on the research results of Wang Shuai [38] et al. and the above experimental results, partial gasification mechanism with air as atmosphere can be explained as follows: with the constant increase of air equivalence ratio and gasification temperature, biochar will continuously capture oxygen from the air to form additional C–O structure, and C–O structure has high reactivity and is easy to be consumed and converted into low reactivity and stable C]O structure, so that the C]O structure is continuously enriched in biochar, thus increasing its relative content. When the air equivalence ratio further increases and the gasification temperature reaches a certain degree, the stable C]O structure will be consumed and decomposed into C–O structure, so that the relative content of C–O structure will rise.

Fig. 12 shows the nitrogen adsorption and desorption isotherms and pore size distributions of biochar from partial gasification under different air equivalence ratios. According to the classification of adsorption isotherms of porous materials, the adsorption isotherms of biochars obtained from the experiments all belong to type II isotherms, which is also consistent with the fact that the macropores are more predominant on the basic of the pore size distribution curve. With the increase of air equivalence ratio and gasification temperature, the adsorption capacity of biochar rose with a little change, which is related to the temperature range. The changes of specific surface area, pore volume and average pore size of biochar partial gasification with different equivalence ratios are shown in Table 6. Excluding the effect of Biochar-2, it can be seen from Table 6 that as the air equivalence ratio

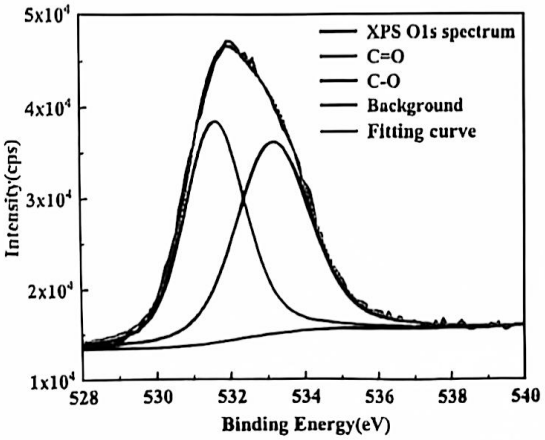

Fig. 11. Peak-differentiating and imitating results of O1s in the original XPS spectrum of biochar.

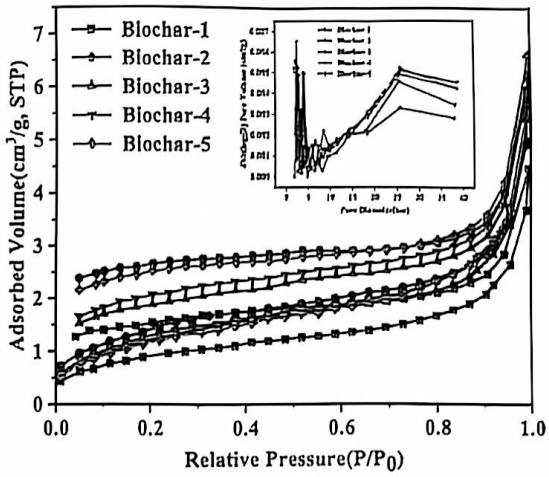

Fig. 12. Adsorption and desorption isotherms and pore size distribution of biochar at different air equivalence ratios.

Table 6
BET surface area, pore volume and average pore size of biochar under different air equivalence ratios.

Items	Biochar-1	Biochar-2	Biochar-3	Biochar-4	Biochar-5
SBET (m^2/g)	3.357	5.246	4.589	4.842	4.398
Vtotal (cm^3/g)	0.006926	0.009214	0.009568	0.01011	0.01025
Daverage (nm)	8.2522	7.0254	8.3406	8.3551	9.3241

increases, the specific surface area keeps rising and then decreases, the pore volume and the average pore size both have a rising trend. It also indicates that with the increase of gasification temperature, more oxygen can enter the internal pores of biochar to promote the partial combustion and gasification reaction, leading to elevate the carbon conversion ratio, which is in accordance with Fig. 7. And the reason why the specific surface area of Biochar-2 reaches 5.246 m^2/g is that H_2O enhances the pore development of biochar, which also explains the different growth rates of gasification efficiency and carbon conversion ratio of the producer gas to biomass in Fig. 5 from another perspective. However, on the whole, the biochars gained from the experiment have a relatively low specific surface area, which may be due to the destruction of partial aromatic hydrocarbon and carbon skeleton by oxidative combustion reaction or the occurrence of internal overpressure and small pore coalescence by the rapid release of volatile components [40, 41].

4. Conclusions

Experiments on biomass partial gasification for biochar and syngas co-production using air as atmosphere are carried out in a self-built small atmospheric bubbling fluidized bed, and the influencing mechanism of air equivalence ratio on gasification performance and biochar characteristics are studied. The main conclusions are as follows: (1) With the air equivalence ratio rises from 0.07 to 0.16, the gasification temperature keeps rising, the combustible gas component content increases first and then decreases, the lower calorific value of wet producer gas keeps decreasing, and the maximum value is 9.16MJ/Nm^3. The gasification efficiency keeps increasing, while the growth rate displays decreasing, indicating the feasibility of partial gasification of biomass. The yield and carbon mass fraction of tar both increase first and then decrease. (2) With the increase of air equivalence ratio, the yield of biochar reduces continuously, the maximum value is 18.07 %, and the

carbon conversion ratio also increases. When the air equivalence ratio is between 0.07 and 0.14, the disorder degree of biochar is improved, mainly due to the newly formation of additional C–O structure. When the air equivalence ratio exceeds 0.14, the gasification temperature reaches a certain level, the biochar becomes orderly gradually.

CRediT authorship contribution statement

Deao Zhu: Methodology, Investigation, Formal analysis, and Writing- Original Draft. **Qinhui Wang:** Conceptualization, Writing – review & editing, Funding acquisition. **Guilin Xie:** Investigation. **Zefu Ye:** Writing – review & editing. **Zhujun Zhu:** Writing – review & editing. **Chao Ye:** Funding acquisition, Writing – review & editing.

Declaration of competing interest

The authors declare that they have no known competing financial interests or personal relationships that could have appeared to influence the work reported in this paper.

Acknowledgments

This research was financially supported by the Science and Technology Innovation Project of Shanxi Gemeng China-US R&D Center and Fundamental Scientific Research Funds for the Central Universities (2022ZFJH004).

References

[1] X. Chen, Economic potential of biomass supply from crop residues in China, Appl. Energy 166 (2016) 141–149.
[2] L. Lang, Y. Chen, Y. Liu, J. Wu, Y. Yu, Y. Wang, X. Chen, Z. Zhang, Changes in spatial patterns of biomass energy potential from biowaste in China from 2000 to 2020, Front. Energy Res. 11 (2023).
[3] Z. Qin, Q. Zhuang, X. Cai, Y. He, Y. Huang, D. Jiang, E. Lin, Y. Liu, Y. Tang, M. Q. Wang, Biomass and biofuels in China: toward bioenergy resource potentials and their impacts on the environment, Renew. Sustain. Energy Rev. 82 (2018) 2387–2400.
[4] P. Dunrah, D. Haldar, A.K. Patel, C.D. Dong, R.R. Singhania, M.K. Purkait, A review on global perspectives of sustainable development in bioenergy generation, Bioresour. Technol. 348 (2022), 126791.
[5] J. He, Y. Liu, B. Lin, Should China support the development of biomass power generation? Energy 163 (2018) 416–425.
[6] Y. Zhang, H. Ma, D. Chen, J. Zhou, Technical and benefit evaluation of fruit-wood waste gasification heating coproduction of an activated carbon system, ACS Omega 6 (1) (2021) 633–641.
[7] J.S. Cha, S.H. Park, S.-C. Jung, C. Ryu, J.-K. Jeon, M.-C. Shin, Y.-K. Park, Production and utilization of biochar: a review, J. Ind. Eng. Chem. 40 (2016) 1–15.
[8] Y. Xie, L. Wang, H. Li, L.J. Westholm, L. Carvalho, E. Thorin, Z. Yu, X. Yu, Ø. Skreiberg, A critical review on production, modification and utilization of biochar, J. Anal. Appl. Pyrol. 161 (2022).
[9] S. You, Y.S. Ok, S.S. Chen, D.C.W. Tsang, E.E. Kwon, J. Lee, C.H. Wang, A critical review on sustainable biochar system through gasification: energy and environmental applications, Bioresour. Technol. 246 (2017) 242–253.
[10] W. Ding, X. Dong, I.M. Ime, B. Gao, L.Q. Ma, Pyrolytic temperatures impact lead sorption mechanisms by bagasse biochars, Chemosphere 105 (2014) 68–74.
[11] X. Xu, X. Cao, L. Zhao, Comparison of rice husk- and dairy manure-derived biochars for simultaneously removing heavy metals from aqueous solutions: role of mineral components in biochars, Chemosphere 92 (8) (2013) 955–961.
[12] T.R. Pacioni, D. Soares, M.D. Domenico, M.F. Rosa, R. Moreira, H.J. Jose, Bio-syngas production from agro-industrial biomass residues by steam gasification, Waste Manag. 58 (2016) 221–229.
[13] Y. Shen, Chars as carbonaceous adsorbents/catalysts for tar elimination during biomass pyrolysis or gasification, Renew. Sustain. Energy Rev. 43 (2015) 281–295.
[14] J. Lee, K.-H. Kim, E.E. Kwon, Biochar as a catalyst, Renew. Sustain. Energy Rev. 77 (2017) 70–79.
[15] K. Poonam, Sharma, A. Arora, S.K. Tripathi, Review of supercapacitors: materials and devices, J. Energy Storage 21 (2019) 801–825.
[16] A. Ellouch, K. Halouani, Y. Li, Investigation of chemical and electrochemical reactions mechanisms in a direct carbon fuel cell using olive wood charcoal as sustainable fuel, J. Power Sources 281 (2015) 350–361.
[17] M. He, X. Xiong, L. Wang, D. Hou, N.S. Bolan, Y.S. Ok, J. Rinklebe, D.C.W. Tsang, A critical review on performance indicators for evaluating soil biota and soil health of biochar-amended soils, J. Hazard Mater. 414 (2021), 125378.
[18] H.P. Schmidt, S. Abiven, C. Kammann, B. Glaser, T. Bucheli, J. Leifeld, et al., European Biochar Certificate - Guidelines for a Sustainable Production of Biochar, European Biochar Foundation (EBC), Arbaz, Switzerland, 2012.
[19] K. Vijayaraghavan, Biochar: production strategies, potential feedstocks and applications, J. Environ. Biotechnol. Res. 4 (2016) 41–49.
[20] X. Zhang, H. Li, L. Liu, C. Bai, S. Wang, J. Zeng, X. Liu, N. Li, G. Zhang, Thermodynamic and economic analysis of biomass partial gasification process, Appl. Therm. Eng. 129 (2018) 410–420.
[21] Z. Yao, S. You, T. Ge, C.-H. Wang, Biomass gasification for syngas and biochar co-production: energy application and economic evaluation, Appl. Energy 209 (2018) 43–55.
[22] J. Rivas, A.M. Carty, Simultaneous Biochar and Syngas Production in a Top-Lit Updraft Biomass Gasifier[D], North Carolina State University, 2015.
[23] Y. Zhang, H. Ma, D. Chen, J. Zhou, Application case analysis of 3MW apricot shell gasification power generation coproduction of activated carbon, heat and fertilizer, Chem. Ind. Eng. Prog. 40 (2021) 1667–1674.
[24] J.-i. Hayashi, S. Kudo, H.-S. Kim, K. Norinaga, K. Matsuoka, S. Hosokai, Low-temperature gasification of biomass and lignite: consideration of key thermochemical phenomena, rearrangement of reactions, and reactor configuration, Energy Fuels 28 (1) (2013) 4–21.
[25] A. Gálvez-Pérez, M.A. Martín-Lara, M. Calero, A. Pérez, P. Canu, G. Blázquez, Experimental investigation on the air gasification of olive cake at low temperatures, Fuel Process. Technol. 213 (2021).
[26] X. Xiao, X. Meng, D.D. Le, T. Takarada, Two-stage steam gasification of waste biomass in fluidized bed at low temperature: parametric investigations and performance optimization, Bioresour. Technol. 102 (2) (2011) 1975–1981.
[27] H. Zhao, Study on Biomass Gasification and Kinetics Based on Real-Time Thermogravimetric Analysis system[D], Xiamen University, 2018.
[28] X. Jia, Q. Wang, K. Cen, L. Chen, An experimental study of CaSO 4 decomposition during coal pyrolysis, Fuel 163 (2016) 157–165.
[29] M.C. Acar, Y.E. Böke, Simulation of biomass gasification in a BFBG using chemical equilibrium model and restricted chemical equilibrium method, Biomass Bioenergy 125 (2019) 131–138.
[30] C. Dupont, R. Chiriac, G. Gauthier, F. Toche, Heat capacity measurements of various biomass types and pyrolysis residues, Fuel 115 (2014) 644–651.
[31] X. Song, Research on Coal Partial Gasification-Based Staged Conversion Technology Co-producing Char Gas Tar in One Fluidized Bed reactor[D], Zhejiang University, 2023.
[32] X. Lu, Study on Coal Partial Gasification & Combustion Integration system[D], Zhejiang University, 2002.
[33] Q. Dun, Z. Chen, F. Huang, Y. Zhou, J. Yu, S. Gao, et al., Influences of temperature and residence time on secondary reactions of volatiles from coal pyrolysis, Chin. J. Process Eng. 18 (2018) 140–147.
[34] X. Li, J. Hayashi, C. Li, FT-Raman spectroscopic study of the evolution of char structure during the pyrolysis of a Victorian brown coal, Fuel 85 (12–13) (2006) 1700–1707.
[35] C. Guizani, K. Haddad, L. Limousy, M. Jeguirim, New insights on the structural evolution of biomass char upon pyrolysis as revealed by the Raman spectroscopy and elemental analysis, Carbon 119 (2017) 519–521.
[36] J. Wei, M. Wang, G. Tang, M.A. Akhtar, D. Xu, X. Song, G. Yu, B. Li, H. Zhang, S. Zhang, Advances on in-situ analysis of char structure evolution during thermochemical conversion of coal/biomass: a review, Fuel Process. Technol. 230 (2022).
[37] S. Wang, L. Wu, X. Hu, L. Zhang, T. Li, S. Jiang, K.M. O'Donnell, C.E. Buckley, C.-Z. Li, Changes in the biochar chemical structure during the low-temperature gasification of mallee biochar in air as revealed with fourier transform infrared/Raman and X-ray photoelectron spectroscopies, Energy Fuels 32 (12) (2018) 12545–12553.
[38] S. Wang, L. Wu, X. Hu, L. Zhang, K.M. O'Donnell, C.E. Buckley, C.-Z. Li, An X-ray photoelectron spectroscopic perspective for the evolution of O-containing structures in char during gasification, Fuel Process. Technol. 172 (2018) 209–215.
[39] Z.-W. Ma, H.-Q. Liu, Q.-F. Lü, Porous biochar derived from tea saponin for supercapacitor electrode: effect of preparation technique, J. Energy Storage 40 (2021).
[40] B.B. Uzun, E. Apaydin-Varol, F. Ateş, N. Ozbay, A.E. Pütün, Synthetic fuel production from tea waste: characterisation of bio-oil and bio-char, Fuel 89 (1) (2010) 176–184.
[41] J. Li, Study on the Gasification of Biomass-Molded Fuel in Fluidized Bed and the Synergistic Effect of Co-combustion of Coke and Coal [D], Huazhong University of Science & Technology, 2020.